29101 DUP

IGM88TC-108-753-G
CNRC 29101

RHEOLOGICAL EVALUATION OF POLYSTYRENE/POLYETHYLENE BLENDS

by

L.A. Utracki and P. Sammut

National Research Council Canada

Industrial Materials Research Institute

75 De Mortagne, Boucherville, Quebec, Canada, J4B 6Y4

Presented at the NRCC/IMRI symposium "Polyblends-'88", Boucherville, Que., Canada, April 5-6, 1988

RHEOLOGICAL EVALUATION OF POLYSTYRENE/POLYETHYLENE BLENDS

L.A. Utracki and P. Sammut, National Research Council Canada, Industrial Materials Research Institute, 75 De Mortagne, Boucherville, Quebec, Canada, J4B 6Y4

ABSTRACT

The dynamic shear behavior at 200°C of low density polyethylene, LDPE, polystyrene, PS, and their blends was studied. Two series of blends were prepared containing LDPE:PS = 1:2, 2:1 and 17:3; the first series contained 0, the second 5 wt% of the compatibilizing, partially hydrogenated poly(styrene-b-isoprene) di-block copolymer, SEB. From the Casson plot the apparent yield stress $G'_y > G''_y$ was found; addition of SEB decreased both these functions, but the inequality remained valid. After subtracting the yield stress values the frequency relaxation spectrum was computed from the G" = G"(ω). The linear viscoelastic functions determined from the spectrum were found to agree with experimental values within a range of error below 5%. The blends were found to be thermorheologically complex with the time-temperature shift factors depending on both temperature and frequency. A compositional dissymmetry of blend morphology was observed: PS dispersed in LDPE formed spheres, while at corresponding concentration LDPE in PS formed fibers. Difference in surface tension of the two polymers, leading to different spreading coefficient $S_{PE/PS} \neq S_{PS/PE}$, or dissymmetry of the interfacial tension coefficient could provide a possible explanation.

INTRODUCTION

Polymer alloys and blends, PAB, constitute one of the most dynamic segments of the plastics industry. Fueled by the commercial interest there is a voluminous literature on various aspects of behavior of these materials. From a practical point of view the more numerous immiscible PAB are of prime interest. Even when a miscible blend is found, its commercial version invariably contains a second phase, either for toughening or for increasing the modulus.

More than 20,000 patents and technical papers are published annually on PAB. However, of this considerable number only a few deal with more fundamental aspects of flow of the immiscible blends. In particular, the knowledge of correlation between the rheological properties and morphology of PAB needs improvement. Since one of the principal means of morphology modification is addition of a compatibilizer, the effect of this ingredient on flow behavior is also of interest.

Recognizing these needs the IUPAC Working Party 4.2.1. on "Structure and Properties of Commercial Polymers" decided to carry out an extensive test program on model blends based on low density polyethylene, LDPE, and polystyrene, PS, with and without the partially hydrogenated poly(styrene-b-isoprene) di-block copolymer, SEB. The work reported in this paper represents part of these studies.

EXPERIMENTAL

1. MATERIAL. The properties of LDPE, PS and SEB are listed in Table 1. The nine samples listed in Table 2 were prepared for the participants in the program by Werner-Pfleiderer Corp., Ramsay, NJ, using a twin-screw extruder, ZSK-30 with the nominal barrel temperature of 200°C, nominal output rate at 10 kg/h, and the screw speed at 250 RPM. Note that blends are identified by the LDPE content (e.g. 33 indicates 33.33 LDPE) and for the presence or absence of 5 wt% SEB, e.g. 33K or 33, respectively. The samples were supplied as pellets. To ascertain a similar thermomechanical history of all samples, the homopolymers were also repelletized.

2. PREPARATION OF THE SPECIMENS. The samples were compression molded at 185 ± 2.5°C using a Carver laboratory press equipped with water cooled platens. Total molding time was 15 min, including cooling at a rate of 20 to 25 °C/min. The dimensions of the resulting disk-shaped specimens were 2 mm thick with diameter of either 25 or 50 mm (to fit the RMS tooling).

3. EQUIPMENT. The dynamic tests were carried out in Rheometrics Mechanical Spectrometer, RMS, model 605 at 200°C using parallel (polished) plates. The rheological behavior of each sample was examined as a function of strain, γ, time, t, and frequency, ω. Prior to testing the samples were dried for at least 16 hrs at 80°C under vacuum. The measurements were performed under a blanket of dry nitrogen. Both size diameter tooling (25 and 50 mm) were used. The storage and loss shear moduli, G' and G" respectively, were measured.

RESULTS

1. STRAIN SWEEP. (T = 200°C, ω = 10 rad/s, step = 2%, test time t = 6.6 min). The effects of strain, γ, on G' for LDPE, PS and SEB is presented in Fig. 1. For all samples the linear viscoelastic region was observed up to a maximum strain γ_m listed in Table 3. For subsequent measurements the values $\gamma_\omega < \gamma_m$ were selected; these are also given in Table 3. Since γ_m depends on the test frequency at γ_ω the linear viscoelastic behavior is assured only at $\omega \lesssim 10$ rad/s.

2. TIME SWEEP. (T = 200°C, ω = 10 rad/s, strain = γ_ω, test time t = 60 min). To illustrate thermal stability of the samples a plot of the most sensitive rheological function, G' vs. t, is shown in Fig. 2. The change of G' during 60 min at 200°C is listed in Table 3. Since the frequency sweep (see below) lasts $t \lesssim 25$ min, the samples can be considered stable.

3. FREQUENCY SWEEP. (T = 200°C, $\omega = 10^{-2}$ to 10^{2} rad/s, strain = γ_ω). For each sample, two sweeps were made; one from $\omega = 10^{-1}$ to 10^{2} with small parallel plates and the second from ω = 1 to 10^{-2} rad/s using larger platens. An excellent reproducibility (±2%) within the overlapping decade of frequency was obtained (see Table 3). In Fig. 3 the frequency sweep results for LDPE and PS are presented. For clarity the data are displaced by two decades in frequency. The dynamic viscosity, η' vs. ω, for all nine samples is shown in Fig. 4.

For blends 33 and 33K the frequency scan from $\omega = 10^{-1}$ to 10^{2} rad/s was

performed at four temperatures: 150, 170, 200 and 240°C. The storage and loss moduli were horizontally shifted in an attempt to generate the time-temperature master curve (the data will be presented in a later part of this paper).

4. MORPHOLOGY. Jeol Model JSM-35CF scanning electron microscope, SEM, was used. The specimens were fractured under liquid nitrogen, mounted on sample holders and coated with gold/palladium. The blends were analyzed: (i) prior to shearing (as prepared), (ii) sheared at $\omega = 0.1$ rad/s for 30 min, and (iii) sheared at $\omega = 10$ rad/s for 18 sec. Examples of the results are shown in Photos 1 and 2.

DISCUSSION

1. APPARENT YIELD STRESS. It is evident from data in Fig. 4 that at low frequency not only SEB, but also most blends show an upturn of η' which can be considered as evidence of a three-dimensional association of the dispersed phase, i.e. of an apparent yield stress, σ_y. The numerical values of σ_y were calculated from the modified Casson equation:

$$F^{\frac{1}{2}} = F_y^{\frac{1}{2}} + \underline{a} F_m^{\frac{1}{2}} \qquad (1)$$

where F and F_m are, respectively, the rheological function of a blend and matrix phase, F_y, is the yield in respect to F and $\underline{a}^2$ is a relative value of F. Both the storage and loss moduli were used to calculate the yield, i.e. F

= G' or G", respectively. For $F = \sigma_{12}$ (the shear stress) $\underline{a}^2$ has a meaning of the relative viscosity, η_r. Since η_r in the thermoplastic blends is seldom independent of the shear rate, $\dot{\gamma}$, by analogy a constant value of $\underline{a}$ should not be expected for F = G' or G". Only those cases in which the changes in G' or G" with frequency in the matrix polymer were paralleled by those of the blend showed a Casson plot with a constant slope, $\underline{a}$.

In Fig. 5 an example of a Casson plot for blends 33 and 33K is shown. It is important to note that for both blends the yield value, F_y, goes to zero when the frequency decreases below $\omega \approx 0.16$ (rad/s). However, for $\omega \geq 0.16$ the F_y is constant, equivalent to the yield stress in the classical sense of the word. The "apparent" character of the yield stress in polymeric systems was discussed by Onogi and Matsumoto [1]. Recently Utracki [2] proposed consideration of the three-dimensional, interactive structure as a dynamic system characterized by two parameters: the high frequency yield stress, F_y, and the mean relaxation time, τ_y:

$$\sigma_y = F_y \{1 - \exp(-\tau_y \omega)\} \qquad (2)$$

Note that for $\omega \to 0$ and $\omega \to \infty$, $\sigma_y \to 0$ and $\sigma_y \to F_y$, respectively. Equation (2) can be added to any F vs. ω dependence providing a full description for systems with an apparent yield stress. For example, it was found [2] that flow behavior of blends and composites with an apparent yield stress can be well described combining Eq (2) with the following dependence proposed earlier [3]:

$$\eta' = \eta_0/[1 + (\omega\tau)^{m_1}]^{m_2} \qquad (3)$$

where the dynamic viscosity, η', is corrected (see Eq (4), below) for the yield stress, η_0 is the zero-shear viscosity, τ is the principal relaxation time and m_1, m_2 are parameters related to polydispersity. The experimentally determined apparent dynamic viscosity can be written as:

$$\eta'_a \equiv G''_a/\omega = (G'' + G''_y)/\omega = \eta' + G''_y/\omega \qquad (4)$$

where G''_a indicates an "apparent" value of the shear loss modulus. The dynamic flow curve can be expressed by combining Eqs (2) to (4).

Returning to Fig. 5, it was noted that for sample 33 the slope was constant, independent of ω for all but the lowest values of the frequency $\omega < 0.16$, where Eq (2) was obeyed. After addition of 5% of SEB to this sample, i.e. in blend 33K, a positive deviation from the straight line appeared for data measured at higher frequency $\omega \geq 20$ rad/s. The point of departure from the linear dependence is indicated as F_m^d. Analogous plots of G''_a for the same samples showed even stronger effect. The change of slope in other samples was observed at lower frequency than that in 33K. It was postulated that the lower limit was due to higher instability of morphology in samples containing PS as the dispersed phase.

Photos 1 and 2 confirmed this postulate. In Photo 1 the SEM micrographs of

blend 66K are presented: (a) prior to testing, after testing for 30 min at $\omega = 0.1$ (b) and for 18 sec at $\omega = 10$ rad/s (c). The samples were taken from edge of the RMS specimens. The average droplet diameter in (a) is $\bar{d} = 1.4 \pm 0.3$ μm, in (b) is $\bar{d} = 2.8 \pm 0.2$ μm and in (c) the PS phase is in a form of short fibers with diameter of about 4 μm and aspect ratio L/D ≈ 5. Obviously, shearing at 200°C at low frequency leads to significant coalescence (doubling droplet diameter), but at 10 rad/s the effect is significantly more pronounced in spite of shorter test time. Similar information is shown in Photo 2 for blend 66. Here, to start with, in absence of SEB, the dispersion was coarser ($\bar{d} \approx 3 \pm 0.5$ μm) coalescing even further during the test (see Photo 2a and 2c where $\bar{d} \approx 8$ μm) and deforming at low as well as high test frequency (Photos 2b and 2d).

The computed values of F_y, τ_y, the slope $\underline{a}$, the correlation coefficient squared, r^2, and the value of F_m^d are listed in Table 4. For the purposes of computation, only the low frequency data (before the onset of positive deviation at F_m^d) were used. The following regularities are to be noted: (i) for G_a' the values of F_y and F_m^d are larger whereas of τ_y are smaller than those for G_a'', (ii) there is a significant difference in magnitude of these three parameters for samples with PS as matrix compared to those in which LDPE is the matrix, (iii) the yield stress of compatibilized samples is smaller than that of the binary LDPE/PS mixtures, and (iv) within the experimental uncertainty neither τ_y nor F_m^d are affected by addition of SEB.

In Fig. 6 the relation between F_y and composition is shown. The relative

magnitude of the yield stress is as follows: $G'_y > G'_y(K) > G''_y > G''_y(K)$, where G'_y, G''_y refer to blends of LDPE/PS and $G'_y(K)$, $G''_y(K)$ to those with 5% SEB. In short, (i) addition of the compatibilizer lowers the yield stress, and (ii) the yield value of the storage modulus is larger than that of the loss modulus. While being cautious not to generalize this observation one should point out that $G'_y > G''_y$ was also reported for polypropylene/mica at 180°C [4]. SEB does not seem to influence either the relaxation time of the three-dimensional structure or the blend deformability at higher frequency.

2. RELAXATION SPECTRUM. It was shown [5] that substituting Eq (3) into Gross' definition of the frequency relaxation spectrum, H_G, leads to:

$$\tilde{H}_G \equiv H_G/\eta_0 = (2/\pi) r^{-m_2} \sin(m_2\theta) \qquad (5)$$

where:

$$r \equiv [1 + 2(\omega\tau)^{m_1} \cos(m_1\pi/2) + (\omega\tau)^{2m_1}]^{\frac{1}{2}}$$

and:

$$\theta \equiv \arcsin\{(\omega\tau)^{m_1} r^{-1} \sin(m_1\pi/2)\}$$

with η_0, τ, m_1 and m_2 - the parameters of Eq (3).

In accord with Eq (4) subtracting the yield value, G''_y, from the apparent G''_a vs. ω data allows calculation of the true η' vs. ω dependence. These values can be analyzed by means of Eq (3) computing the equation parameters by the least squares non linear computer fit method (the curves in Fig. 4 represent

the computed dependencies with the parameters listed in Table 5). Once the four parameters are known the relaxation spectrum and then any linear viscoelastic function can be in turn computed.

There are two limiting values to η' in Eq (3). For $\omega \to 0$ the dynamic viscosity, $\eta' \to \eta_0$; for large values of $(\omega\tau)^{m_1} \gg 1$, Eq (3) can be written in a form of the power-law dependence:

$$\eta' = \kappa\omega^{n-1} = \eta_0/(\omega\tau)^{m_1 m_2} \qquad (6)$$

i.e. $n = 1 + m_1 m_2$. Since $0 \lesssim n \lesssim 1$ also $0 \lesssim m_1 m_2 \lesssim 1$ giving the second limiting value of the dependence. The data in Table 5 indicate that both limits were indeed observed.

In Fig. 7 the Cole-Cole plot for the homopolymers and blends is shown in a reduced form: η''_a/η_0 vs. η'_a/η_0 or η''/η_0 vs. η'/η_0, where η_0 is taken from Table 5. Since the axes in this Figure are linear with the curves intersecting the abscissa at 0 and 1 the accuracy of η_0 is judged to be better than ± 10%. In Figs. 7a and 7c the apparent dynamic viscosities, η'_a and η''_a, were used without correcting them for the apparent yield stress. By contrast, in Figs. 7b and 7d, the corrected values of η' and η'' were used. Figs. 7a and 7b present behavior of the two component LDPE/PS systems, while Figs. 7c and 7d illustrate those containing 5 wt% of SEB. In all four graphs the curves for homopolymers are the same. Comparing the graphs horizontally, Fig. 7a with 7b

and 7c with 7d, the effect of the yield is visible; F_y tends to add another relaxation peak at high values of η', i.e. at low frequency. After subtracting it the curves became more symmetrical, resembling those of matrix polymer. Comparing the graphs vertically a small effect of SEB addition is to be noted.

The theories of linear viscoelastic behavior indicate that the cross-point coordinates:

$$G_x \equiv G' = G'' \quad \text{at} \quad \omega = \omega_x$$

are related to the zero-shear viscosity [6]:

$$\eta_{oM} = A(G_x/\omega_x) \tag{7}$$

where A = 2 or $\pi^2/3$ for the single relaxation Maxwell or Rouse model, respectively. Eq (7) was found to be obeyed by the linear low density polyethylenes, polypropylenes and their blends [7, 8] with $\eta_0 \lesssim 50$ kPas; for higher viscosities the multiple relaxations were found to reduce A by a factor of up to 7. For polymers with the same polydispersity Eq (7) predicts that η_0 should be inversely proportional to ω_x [9]. The experimental values of (G_x, ω_x) are listed in Table 5. Except for the homopolymers and blend 33, the results for other samples disagree with both Eq (7) as well as the predicted proportionality: $\eta_0 \propto 1/\omega_x$. It seems that indeed at low and high

frequencies there are two blend morphologies, with different rheological properties; the value of η_0 computed at $\omega \to 0$ is unrelated to (G_x,ω_x) determined at higher frequency. However, the (G_x,ω_x) data are self-consistent; the plot of G_x vs. ω_x is linear:

$$G_x(\text{kPa}) = 7.75 + 3.00\omega_x \qquad \text{with} \qquad r^2 = 0.996.$$

The compositional variations of (G_x,ω_x) and η_0 for the two component LDPE/PS blends are shown in Figs. 8 and 9, respectively. The data points for blend with PS as a matrix are located on the log-additivity line, whereas those for LDPE as a matrix follow a strong positive deviation curve. The deviation is much stronger for η_0 than for the two other higher frequency functions. The high value of η_0 is unrelated to the yield stress (subtracted from G''_a prior to η_0-computation) and represents the effect of dispersing the immiscible PS-phase in LDPE matrix. It is worth noting that even although Eq (7) is not numerically obeyed qualitatively ω_x vs. LDPE content is a mirror image of the data in Fig. 9.

An example of computation of the dynamic shear moduli is shown in Fig. 10. Since these are based on Eqs (3) and (4), the fit to G" vs. ω should first be examined. The main question is whether in spite of the morphological changes at higher frequency these equations can be used to describe the G" (or η') dependence on frequency. The answer seems to be affirmative; the maximum difference between the experimental and computed values is $\Delta G''(\%) = 4.4$ at $\omega = 100$ rad/s. Next, the G' vs. ω should be analyzed. The computed values of G' in Fig. 10 (lines) were calculated from the dependence [10]:

$$G'(\omega) = \int_{-\infty}^{+\infty} [sH_G(s)/[1+(s/\omega)^2]]d\ln s \qquad (8)$$

where $H_G(s)$ is the Gross frequency relaxation spectrum computed from G" data by means of Eq (5). It can be seen that in Fig. 10 the computed curves well represent the experimental $G'(\omega)$ data; the maximum difference $\Delta G'(\%) = 3.5$ was calculated at $\omega = 100$ rad/s. Similarly, from H_G any other linear viscoelastic function can be calculated.

In Fig. 11 the computed Gross frequency relaxation spectra are shown for samples without (a) and with (b) SEB. In accord with the molecular weights the spectrum for LDPE is significantly broader than that for PS. For blends 33 and 33K the spectra are nearly identical, lying half-way between those of homopolymers. The curves for the remaining blends, in which LDPE is the matrix, are significantly broader, especially in the low frequency region. It is worth noting that addition of high-viscosity compatibilizer, SEB, narrows the spectrum. It seems that these low frequency events are related to slow relaxation processes associated with the morphological changes. Near the phase inversion composition, blends 66 and 66K, these processes are particularly slow. The relative stability of the mechanically interlocked co-continuous polymeric structures near the phase inversion has been reported by Maxwell and his collaborators for PS blends with polymethylmethacrylate [11] or with polyethylene [12]. In the latter case the 50:50 blend did not show significant ripening after 3 hrs at 180°C.

3. TIME-TEMPERATURE SUPERPOSITION. There are severe experimental difficulties in measuring the viscoelastic properties over extended time, t, or temperature, T, range. For this reason the method of tT-superposition has been frequently used [10]. The method can be applied only to systems with stable morphology within the range of measured variables. There are several sources of difficulties in generating a tT-master curve for semi-crystalline polymers at $T \lesssim T_m$, or even for amorphous polymers scanned accross T_g (T_m and T_g are respectively melting and glass transition temperature). However, for the homogeneous melts the tT-superposition provides a simple and straightforward extension of experimental variables.

There are numerous reports on tT-superposition for polymer blends [6]. When the morphology is stable (either by virtue of miscibility, rigidity or stabilization of the dispersed phase) the method works quite well. For the studied system, as stated before, the morphology is not stable and there are the yield stresses in G'_a as well as in G''_a. For this reason, here the tT-superposition is not to be expected. However, in sample 33 at 200°C there was no indication of modification of morphology in the full range of ω, which could possibly lead to superposability. It was decided to examine if the tT-master curve can be constructed for this rheologically simplest blend.

The dynamic-mechanical properties were examined within three decades of frequency (ω = 0.1 to 100 rad/s) at T = 150, 170, 200 and 240°C. The data were superimposed by horizontal shifting of G'_a (see Fig. 12). Since these data were not corrected for the yield stress, superposition at high frequency

was emphasized. Using the experimental (determined for G'_a) horizontal shift factor $a_T = a_T(T, \omega=100)$, the G''_a values are plotted vs. ωa_T in Fig. 13.

The two sets of G'_a and G''_a data determined at 200 and 240°C superposed very well in the full range of frequency. However, those measured at 170 and 150°C showed quite a different behavior, with strong deviation at low frequency due to yielding. In addition, in Fig. 13, a deviation of G''_a (150°C) data at high frequency is quite apparent. By analogy with data for other samples the latter deviation is most likely due to morphology modification at a higher stress/straining rate . It is obvious that for blend 33 the assumption of a_T independency of time (or frequency) at $T < 200$°C is unjustified. In consequence the LDPE/PS blends are found to be thermorheologically complex, unable to follow the tT-master curve [13].

The $a_T = a_T(T, \omega=100)$ vs. T dependence is shown in Fig. 14. The three curves represent the following dependencies respectively:

1. Arrhenius [14]: $$\ln a_T = A + \Delta H_\eta / RT \qquad (9)$$

2. WLF [9]: $$\log a_T = -c_1^0(T-T_s)/(c_2^0 + T-T_s) \qquad (10)$$

with universal constants: $c_1^0 = 8.86$ and $c_2^0 = 101.6$; and

3. Utracki [15]: $$\ln a_T = B_0 + B_1 Y \qquad (11)$$

where: $$Y \equiv 1/[h \exp\{0.1151(T/T_g)^{3/2}\} - 1]$$

The least-squares fit of data to Eq (9) gave the activation energy of flow ΔH_η = 89.6 kJ/mole and the correlation coefficient squared, r^2 = 0.997. The WLF Equation (10) with the universal constants and T_s = 200°C (in order that a_T = 1 at the reference temperature) fits quite poorly. A much better result was obtained treating Eq (10) as a three parameter equation. Optimization of parameters led to : c_1^0 = 4.73, c_2^0 = 235.7 and T_s = 200°C with r^2 = 0.999. Finally, Eq (11) was used assuming that the shielding parameter h = 0.98 and T_g = 100°C (the values determined independently for the matrix polymer, PS). Eq (11) provided the best description of the a_T vs. T dependence. The values of h and T_g were taken to be identical to those of PS.

While curve 2 in Fig. 9 represents data from this work, curve 1 was drawn for η_0 of LDPE/PS mixtures at 200°C reported by Bolotnikova et al. [16]. The η_0's were also obtained by extrapolating η' to $\omega \to 0$. While the two curves differ in absolute value of η_0 they agree in overall behavior. By contrast, the capillary flow data at constant shear rate, $\dot{\gamma}$, or stress, σ_{12}, show strong negative deviation from the log-additivity rule [17, 18]. The fundamental difference between steady state and dynamic shear measurements is the magnitude of strain. The difference in information provided by these two types of measurements reflects on morphological differences of sheared blends.

It is interesting that PS blends with high density polyethylenes, HDPE/PS behaved differently than those of LDPE/PS; the steady state viscosities (at constant shear stress) when plotted vs. concentration showed a sigmoidal dependence with the positive deviation for HDPE-rich blends [17, 19-21]. The magnitude of the negative deviation from the log-additivity decreased with increase of σ_{12}. As a result, the η vs. concentration dependence at high shear stress approached the shape of curves in Fig. 9.

The morphology of LDPE/PS or HDPE/PS has been analyzed [21-24]. Early on it was recognized that in these systems morphology is not "symmetrical", i.e. while at 20% of PS in polyethylene the droplets were formed, under analogous conditions at 20% of polyethylene in PS the fibers predominated. This is in accord with the observation reported in Photos 1 and 2. Both, van Oene [22] and Starita [23], using different arguments, blamed the morphological dissymmetry on the differences in normal stresses of the two homopolymers. The effect also resembles those known in colloid science as dissymmetry of the spreading coefficients, $S_{A/B} \equiv \nu_B - \nu_A - \nu_{AB} \neq S_{B/A}$, or (less frequent) inequality of the interfacial coefficients, $\nu_{AB} \neq \nu_{BA}$. For LDPE/PS blends either $S_{L/S} > S_{S/L}$ (which leads to $\nu_S < \nu_L$) or $\nu_{SL} < \nu_{LS}$, where S and L stand for PS and LDPE, respectively, the first symbol representing the dispersed polymer, the second the matrix. For HDPE/PS blends the interfacial tension seems to be higher than that in LDPE/PS system. This leads to interlayer slip [18] and the negative deviation from the log-additivity rule, i.e. $\nu_{SL} < \nu_{LS} < \nu_{SH} < \nu_{HS}$. While the argument based on the spreading coefficient is quite satisfactory and it leads to

correct inequality [24], it is less convenient to use in comparing two blend types. On the other hand, the inequality of the interface coefficients in polymer blends has been postulated [25] but never measured.

Sjoerdsma et al. [26] reported that addition of 1% of partially hydrogenated poly(styrene-b-butadiene) had a profound effect on bonding the LDPE droplets to PS matrix. Indeed, at low temperatures, $T \lesssim -120°C$, the negative deviation in G' vs. composition (minimum of 30% observed at 35% LDPE) considered by the authors as due to poor interphase adhesion, entirely disappeared upon addition of the compatibilizer. The blends discussed in this paper do not seem to enjoy similarly strong benefits by addition of 5% SEB. As demonstrated in Figs. 4, 7 and 11 the SEB effects on <u>overall</u> blend response are minor; only the droplet size and the yield stresses are significantly reduced. One may suspect that not all 5% of SEB are on the interface. Probably most of it is dispersed in the homopolymer phase - judging by the data in Table 1 primarily in LDPE.

CONCLUSIONS

The LDPE/PS system is immiscible with relatively large values of the apparent yield stress in storage and loss moduli. The "apparent" nature can be characterized by the long relaxation time of the associated structures, τ_y = 132 to 4150 (sec). Addition of SEB reduces the yield stresses. After subtracting the yield stress the rheological properties of blends with PS as matrix are additive, while those with LDPE a matrix show higher than predicted η_0.

The relaxation spectrum was computed using corrected for the yield stress η' vs. ω data at 200°C. The spectrum shows a non-additive broadening for blends 66, 66K, 85 and 85K; larger for 66 and 85, smaller for blends with the compatilizer. Computed from the relaxation spectra values of G' agreed with measured ones with error smaller than 4%.

For most blends a change of morphology at higher frequency was observed. This instability of structure, accentuated by lowering the temperature, precluded time-temperature superposition. The horizontal shift factor, a_T, was found to depend on both time and temperature. Its high frequency values, $a_T(T, \omega=100)$, were found to be best described by the free volume-based Utracki's equation.

Dissymmetry of morphology as a function of composition for LDPE/PS blends has been reported. In the past, the explanations for this behavior were based on the difference between values of the first normal stress coefficient of the two homopolymers. It was shown that either the concept of spreadability or inequality of the interface tension coefficient may provide an alternative explanation.

ACKNOWLEDGEMENT

The authors wish to thank the IUPAC Working Party 4.2.1 for permission to publish this material as well as express their gratitude to Mr. Michel Thibodeau from NRCC/IMRI for the SEM measurements.

NOTATION

A	- parameter in Eq (7).
a_T	- horizontal time-temperature shift factor.
$\underline{a}$	- slope in Eq (1).
C_i^0	- parameters in WLF Eq (10).
F, F_y, F_m, F_m^d	- a rheological function ($F = G'$, G'', σ_{12},...) its yield value, magnitude in the matrix polymer and at point of deviation in the Casson Eq (1).
G', G'', $G'(K)$, $G''(K)$	- storage and loss shear moduli and their values for samples with SEB (Pa).
h	- shielding parameter in Eq (11).
H_G, $\tilde{H}_G$	- Gross frequency relaxation spectrum and its reduced value.
HDPE	- high density polyethylene.
LDPE	- low density polyethylene.
m_1, m_2	- polydispersity parameters in Eq (3).
n	- power law exponent; Eq (6).
PS	- polystyrene.
r	- functional in Eq (5).
r^2	- correlation coefficient squared.
s	- current variable in relaxation spectrum, Eq (8).
$S_{A/B}$	- spreading coefficient of fluid B on the surface of fluid A
SEB	- partially hydrogenated poly(styrene-b-isoprene).
T	- temperature (°C).

T_g, T_m - glass transition temperature and melting point, respectively.

t - time.

T_s - reference temperature in WLF Eq (10).

$Y = Y(T)$ - function in Eq (11)

γ, γ_m γ_ω - strain (%), its maximum value for linear viscoelastic response and magnitude used in experiments.

$\dot{\gamma}$ - rate of shear straining (s^{-1}).

$\Delta G'$, $\Delta G''$ - difference (%) between measured and computed G', G"

ΔH_η - activation energy; Eq (9).

η, η_0, η_r - viscosity, its zero-shear and relative values (Pa·s).

θ - functional in Eq (5).

$\kappa \equiv \eta(\dot{\gamma}=1)$ - parameter in power law Eq (6).

ν_A, ν_{AB} - surface and interface tension coefficient.

σ_{12} - shear stress (Pa).

$\sigma_y = \sigma_y(t)$ - apparent yield stress.

τ, τ_y - relaxation time and its value for yield cluster; Eqs (3) and (2), respectively.

ω - frequency (rad/s).

Subscripts

A, B, ... - liquid.

A/B - A dispersed in B.

G - Gross.

a	- apparent.
g	- glass.
m	- matrix, maximum, melt.
0	- zero shear.
r	- relative.
s	- reference.
x	- cross point coordinate.
y	- yield.
η	- viscosity.
ω	- experimentally used.

REFERENCES

1. S. Onogi and T. Matsumoto, Polym. Eng. Rev., 1, 45 (1981).
2. L.A. Utracki, S.P.E. Techn. Papers, 34, 1192 (1988); Polym. Eng. Sci., 28, 0000 (1988).

   L.A. Utracki, in "Current Topics in Polymer Science", Vol. 2, R.M. Ottenbrite, L.A. Utracki and S. Inoue, Eds., Hanser Verlag, München (1987).
4. L.A. Utracki, Polym. Compos., 7, 274 (1986).
5. L.A. Utracki and B. Schlund, Polym. Eng. Sci., 27, 1512 (1987).
6. L.A. Utracki, "Industrial Polymer Blends and Alloys", Hanser Verlag, München (1988).
7. L.A. Utracki and B. Schlund, Polym. Eng. Sci., 27, 1512 (1987).
8. M.M. Dumoulin, PhD thesis, Ecole Polytechnique, Montreal (1988).
9. G.R. Ziechner and P.D. Patel, 2nd World Cong. Chem. Eng., Montreal, October, 1981.
10. J.D. Ferry, "Viscoelastic Properties of Polymers", 3rd Edition, J. Wiley and Sons, New York (1980).
11. B.A. Thornton, R.G. Villasenor and B. Maxwell, J. Appl. Polym. Sci., 25, 653 (1980).
12. B. Maxwell, paper presented at the S.P.E. Nat'l. Techn. Conf., Bal Harbour, FL, October 25-27 (1982).
13. D.G. Fesko and N.W. Tschoegl, J. Polym. Sci., 35C, 51 (1971).
14. S. Arrhenius, Z. Phys. Chem., (Leipzig), 1, 285 (1887).
15. L.A. Utracki, J. Macromol. Sci.-Phys., B18, 725 (1980).
16. L.S. Bolotnikova, A.K. Evseev, Yu.N. Panov, and S.Ya Frenkel, Vysokomol. Soed., 24B, 154 (1982).

17. B.-L. Lee and J.L. White, Trans. Soc. Rheol., 19, 481 (1975).

18. C.-C. Lin, Polym. J., 11, 185 (1979).

19. C.D. Han and Y.W. Kim, Trans. Soc. Rheol., 19, 245 (1975).

20. T. Nishimura, Rheol. Acta, 23, 617 (1984).

21. K. Min, J.L. White and J.F. Fellers, J. Appl. Polym. Sci., 29, 2117 (1984).

22. H. van Oene, J. Colloid Interface Sci., 40 448 (1972).

23. J.M. Starita, Trans. Soc. Rheol., 16, 339 (1972).

24. J. Brandrup and E.H. Immergut, Eds., "Polymer Handbook", J. Wiley and Sons, New York (1966).

25. A. Sakanishi and Y. Takano, Jap. J. Appl. Phys., 13, 882 (1974).

26. S.D. Sjoerdsma, J. Dalmolen, A.C.A.M. Bleijenberg and D. Heikens, Polymer, 21, 1469 (1980).

Discussion: L.A. UTRACKI and P. SAMMUT

T.A. HUANG: How did you remove the samples from RMS for the morphological studies?

P. SAMMUT: We cooled down the platens, unscrew them and quench in liquid nitrogen.

T.A. HUANG: You can shut off the heat and then cool with the liquid nitrogen on the instrument. In 3 minutes you can cool down from 200°C to ambient temperature.

M. FAIRLY: Can you comment on significance of a_T in the absence of superposition.

L.A. UTRACKI: In rheologically complex system a_T depends not only on temperature but also on frequency $a_T = a_T(T,\omega)$. In principle the shift factor was calculated at ω = 100 rad/s. I said "in principle" since at T = 200 and 240°C the superposition was obtained in the full range of frequency. At lower temperatures the deviation at low frequency was assumed to be due to presence of the independently determined apparent yield stress Fy. At high stress level existing at high frequency the influence of yield stress is negligibly small. In consequence $a_T = a_T(T,100)$ can be treated as any a_T factor.

A. RUDIN: You both made a point calling it "an apparent" yield stress,

which may indicate that you have a limited faith in it. Can you explain why you used Casson plot and how much faith you have in the calculated values.

L.A. UTRACKI: We are using the adjective "apparent" for indicating the time-dependency of the yield phenomena in the studied blends. The dissipative structure is probably due to interacting dispersed droplets, which under stress must deform flowing one past another. This mechanism explains why in blends with SEB the smaller droplets flow easier resulting in smaller values of F_y. However, I think that the phenomenon is a general one and it will be observed when the τ_y and time of the experiment are comparable. We have confidence in our values of F_y determined from the modified Casson equation. They compared quite well with directly measured F_y's using elongational and/or compressional stresses.

Table 1. PROPERTIES OF THE BLEND COMPONENTS

No.	Properties	Units	LDPE	PS	SEB (a)
1.	Manufacturer	-	BP Chem.	BP Chem.	Shell Chem.
2.	Grade	-	BP33(SZ7772)	HH101 (200200NAW)	Kraton G 1701 (EBF 1553)
3.	Density 25°C	kg/m^3	918	1055	920
4.	Melt flow index	g/10 min	0.26	0.33	0.55
5.	Molecular weight, weight average, $\overline{M}_w$	kg/mole	297	244	N/A
6.	Number average, $\overline{M}_n$	kg/mole	18	134	N/A
7.	$\overline{M}_w/\overline{M}_n$	-	17	2	N/A
8.	Crystallinity	%	52	-	-

Note: N/A stands for "not available"; (a) - according to the manufacturer the molecular weight of SEB is M_w(PS) - M_w(EB) = 76 - 130, and the composition (wt%) PS: EB = 37:63.

Table 2. COMPOSITION OF IUPAC LDPE/PS BLENDS

NO	CODE	COMPOSITION (wt%)		
		LDPE	PS	SEB
1	LDPE	100	-	-
2	PS	-	100	-
3	SEB	-	-	100
4	Sample 33	33.33	66.67	-
5	Sample 33K	32.30	62.70	5.00
6	Sample 66	66.67	33.33	-
7	Sample 66K	62.70	32.30	5.00
8	Sample 85	85.00	15.00	-
9	Sample 85K	81.00	14.00	5.00

Table 3. RHEOLOGICAL PARAMETERS OF IUPAC LDPE/PS SAMPLES

NO	PARAMETER	SYMBOLS (units)	SAMPLES								
			1	2	3	4	5	6	7	8	9
			LDPE	PS	SEB	33	33K	66	66K	85	85K
1	Maximum strain in linear viscoelastic region	γ_m(%)	20	14	4	12	12	12	16	12	14
2	Strain used	γ_ω(%)	15	10	4	10	10	10	10	10	10
3	Change of G' in 60 min	$\Delta G'$(%)	-4.9	-1.3	-5.9	3.0	-0.5	2.4	1.5	1.4	0.7
4	Average error of measurements:										
a	ω-sweep in two directions with small and large plates	%	1.4	1.7	2.8	1.0	1.2	2.9	0.6	1.2	0.6
b	γ sweep vs. ω sweep	%	1.7	2.6	0.2	0.8	3.5	0.8	0.6	0.1	0.8
c	ω sweep vs. time sweep	%	0.0	2.3	4.9	0.7	3.3	0.6	0.8	0.2	0.8
d	γ sweep vs. time sweep	%	1.6	0.3	4.8	0.1	0.2	0.3	0.2	0.0	0.0
e	Total average	%	1.2	1.7	3.2	0.7	2.1	1.2	0.6	0.4	0.6

Table . THE YIELD STRESS PAMARETERS

No.	Sample	Modulus	F_y (Pa)	τ_y (s/rad)	slope,	r^2	Matrix	F_m^d (kPa)
4	33	G'	429	21	0.881	0.9999	PS	>710
	33	G"	187	129	0.863	0.9999	PS	397
5	33K	G'	346	25	0.894	0.9999	PS	624
	33K	G"	151	158	0.879	0.9999	PS	348
6	66	G'	195	223	0.895	0.9998	LDPE	84
	66	G"	32.6	638	0.932	0.9998	LDPE	55
7	66K	G'	229	165	0.858	0.9989	LDPE	96
	66K	G"	47.9	579	0.929	0.9995	LDPE	60
8	85	G'	240	157	0.929	0.9996	LDPE	84
	85	G"	57.2	660	0.956	0.9998	LDPE	70
9	85K	G'	89.3	256	0.964	0.9999	LDPE	130
	85K	G"	33.2	649	0.971	0.9998	LDPE	90

Table 5. RHEOLOGICAL PARAMETERS OF LDPE/PS/(SEB) BLENDS

No.	Sample	η_0 (kPa·s)	τ (s/rad)	m_1 (-)	m_2 (-)	G_x (kPa)	ω_x (rad/s)
1	LDPE	102	8.45	0.407	1.91	12.9	1.87
2	PS	21.4	0.564	0.733	1.25	29.0	7.21
3	SEB	-	-	-	-	-	-
4	33	36.4	1.06	0.530	1.70	21.6	4.35
5	33K	35.0	0.965	0.530	1.69	23.8	5.17
6	66	277	0.894	0.226	4.85	11.9	1.40
7	66K	178	0.673	0.250	4.34	15.7	2.20
8	85	340	4.18	0.199	5.00	11.0	1.06
9	85K	237	4.46	0.211	4.54	12.7	1.53

LEGE[illegible] FOR FIGURES

Fig. 1 Strain sweep at 200°C for partially hydrogenated poly(styrene-b-isoprene), SEB, polystyrene, PS, and low density polyethylene, LDPE. Storage modulus, G', vs. strain, γ, is shown. The arrows indicate the maximum value of $\gamma = \gamma_m$ for the linear viscoelastic response.

Fig. 2 Time sweep at 200°C for SEB(1), PS(2) and LDPE(3). G' at frequency ω = 10 rad/s is shown.

Fig. 3 Frequency sweep at 200°C for PS and LDPE. The storage and loss moduli, G' and G" respectively, as well as complex viscosity, $\eta^* = (G'^2 + G''^2)^{\frac{1}{2}}/\omega$, are plotted vs. ω. Note the different axes for the two polymers.

Fig. 4 Dynamic viscosity, $\eta'_a = G''_a/\omega$, vs. ω at 200°C for samples without (upper curves) and with SEB. Composition of the samples is given in Table 2.

Fig. 5 Modified Casson plot, Eq (1), for storage modulus of blends 33K and 33 (with and without SEB, respectively). Note that $F = G'_a$ and for F_m the G' of matrix polymer, PS, was taken. The yield stress was calculated from the initial straight-line portion of the dependence, below the $(G'_{PS})^{\frac{1}{2}}$ value, marked as F^d_m. The curved portion starting at the origin was computed from Eq (2).

Fig. 6 The yield stress vs. composition for LDPE/PS blends. Curves 1 and 2 refer to yield in G'_a for blends without and with SEB, respectively, whereas curves 3 and 4 refer to yield in G''_a for the same blends. Points - experimental, lines - drawn to help the eye.

Fig. 7 The reduced Cole-Cole plot of: (a and c) apparent data for blends without and with SEB, respectively and for (b and d) corrected for the

yield stress data of the same systems.

Fig. 8 Cross-point coordinates at 200°C vs. LDPE content for blends without SEB.

Fig. 9 Zero-shear viscosity at 200°C vs. LDPE content for two component LDPE/PS blends. Data from [16] are also shown.

Fig. 10 Comparison between computed from the relaxation spectrum (lines) and measured (points) values of the shear moduli for LDPE/PS blends.

Fig. 11 Reduced frequency relaxation spectrum for (a) two component LDPE/PS blends, and for those with 5 wt% of SEB (b).

Fig. 12 Attempt of generation of the time-temperature superposition of apparent storage modulus, G'_a, for blend 33 at T = 150, 170, 200 and 240°C by horizontal shifting. Note good superposition for data at 200 and 240°C and lack of it at 150 and 170°C. The $a_T = a_T(T, \omega=100)$ was determined.

Fig. 13 Time-temperature superposition of the apparent loss modulus, G''_a, for blend 33 obtained by plotting its values vs. ωa_T, where a_T is the empirical shift factor determined in Fig. 12.

Fig. 14 Temperature dependence of the experimental shift factor, $a_T = a_T(T, \omega=100)$, for blend 33 (points). The curves 1 to 3 represent the best fit of the Arrhenius, WLF and Utracki equation, respectively.

Photo 1 The scanning electron micrographs of blend 66K at rim of the RMS specimen: (a) prior to testing, (b) after 30 min at ω = 0.1 rad/s, T = 200 °C, and (c) after 18 sec at ω = 10 rad/s, T = 200°C.

Photo 2 The scanning electron micrographs of blend 66 at the center of RMS parallel plates geometry (top) and at the edge. The test frequency was ω = 0.1 (left) and ω = 10 (rad/s) right.

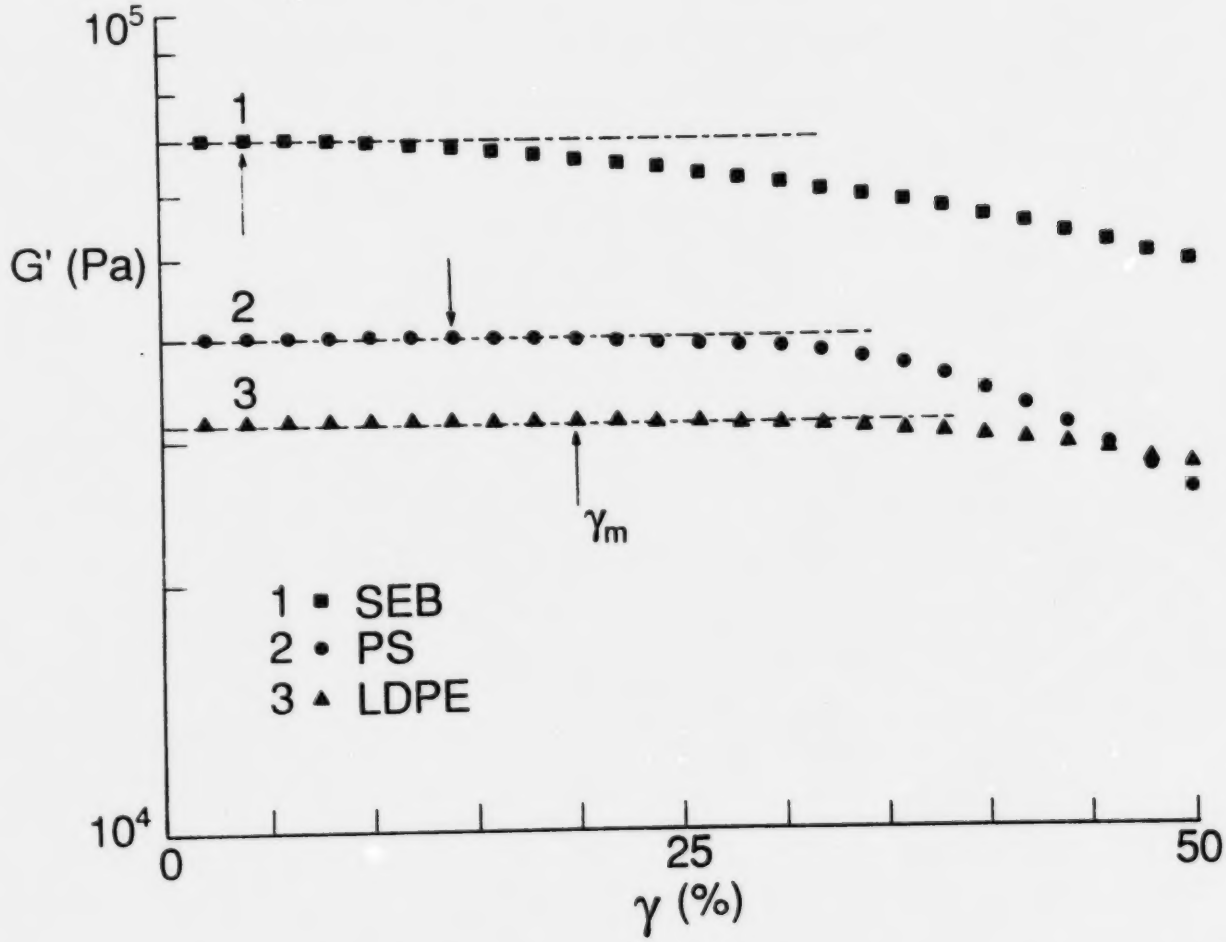

Fig. 1 Str[illegible] sweep at 200°C for partially hydrogenated poly(styrene-b-iso[illegible]ne), SEB, polystyrene, PS, and low density polyethylene, LDPE. Storage modulus, G', vs. strain, γ, is shown. The arrows indicate the

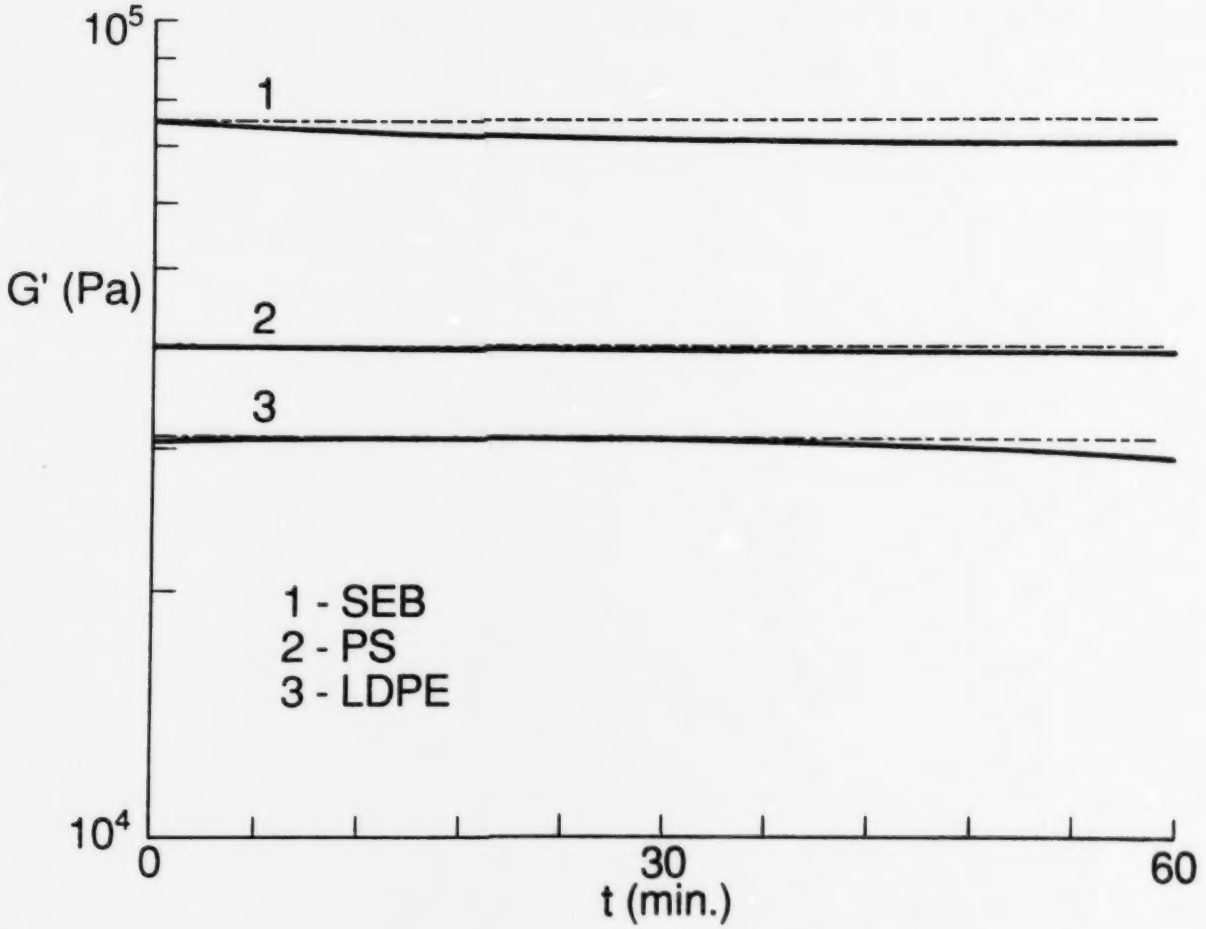

Fig. 2 Time sweep at 200°C for SEB(1), PS(2) and LDPE(3). G' at frequency ω = 10 rad/s is shown.

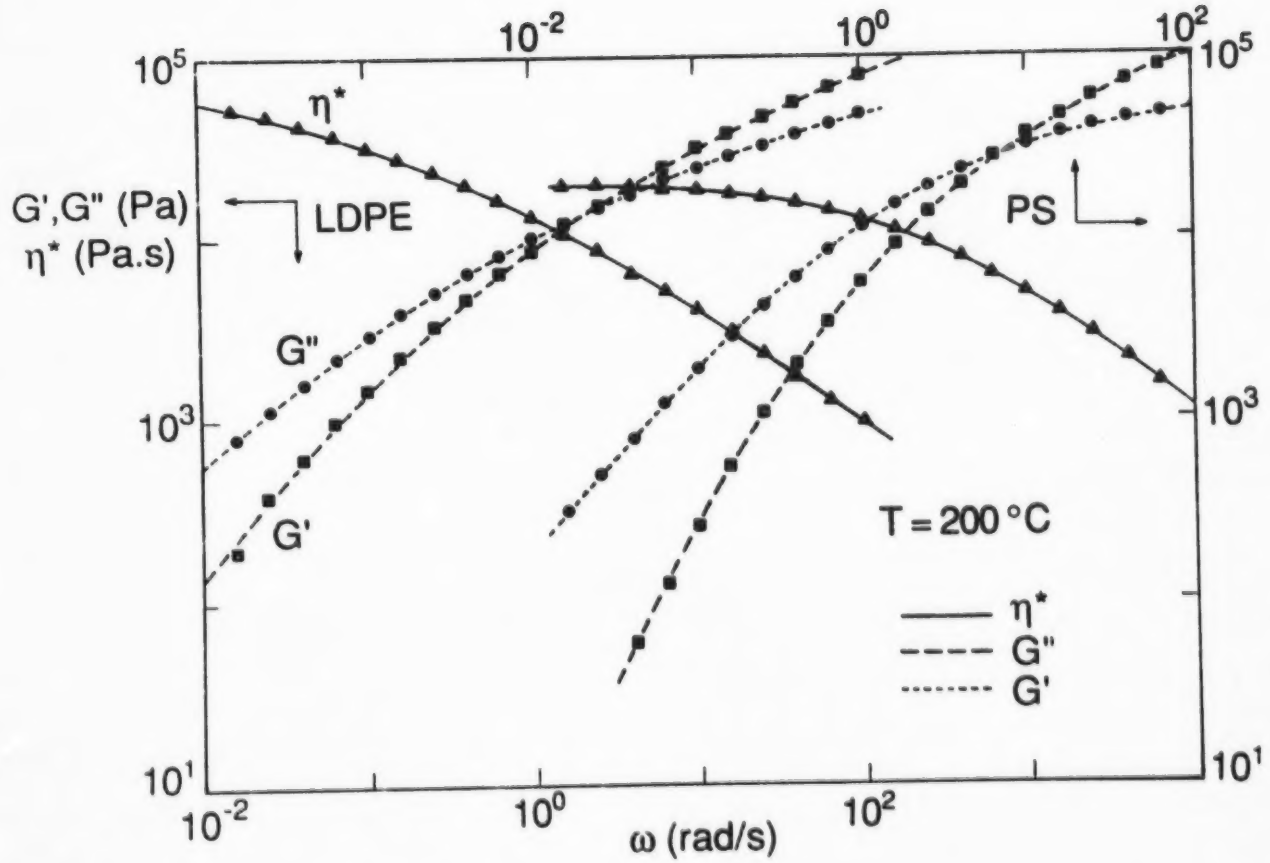

Fig. 3 Frequency sweep at 200°C for PS and LDPE. The storage and loss moduli, G' and G" respectively, as well as complex viscosity, $\eta^* = (G'^2 + G''^2)^{\frac{1}{2}}/\omega$, are plotted vs. ω. Note the different axes for the two polymers.

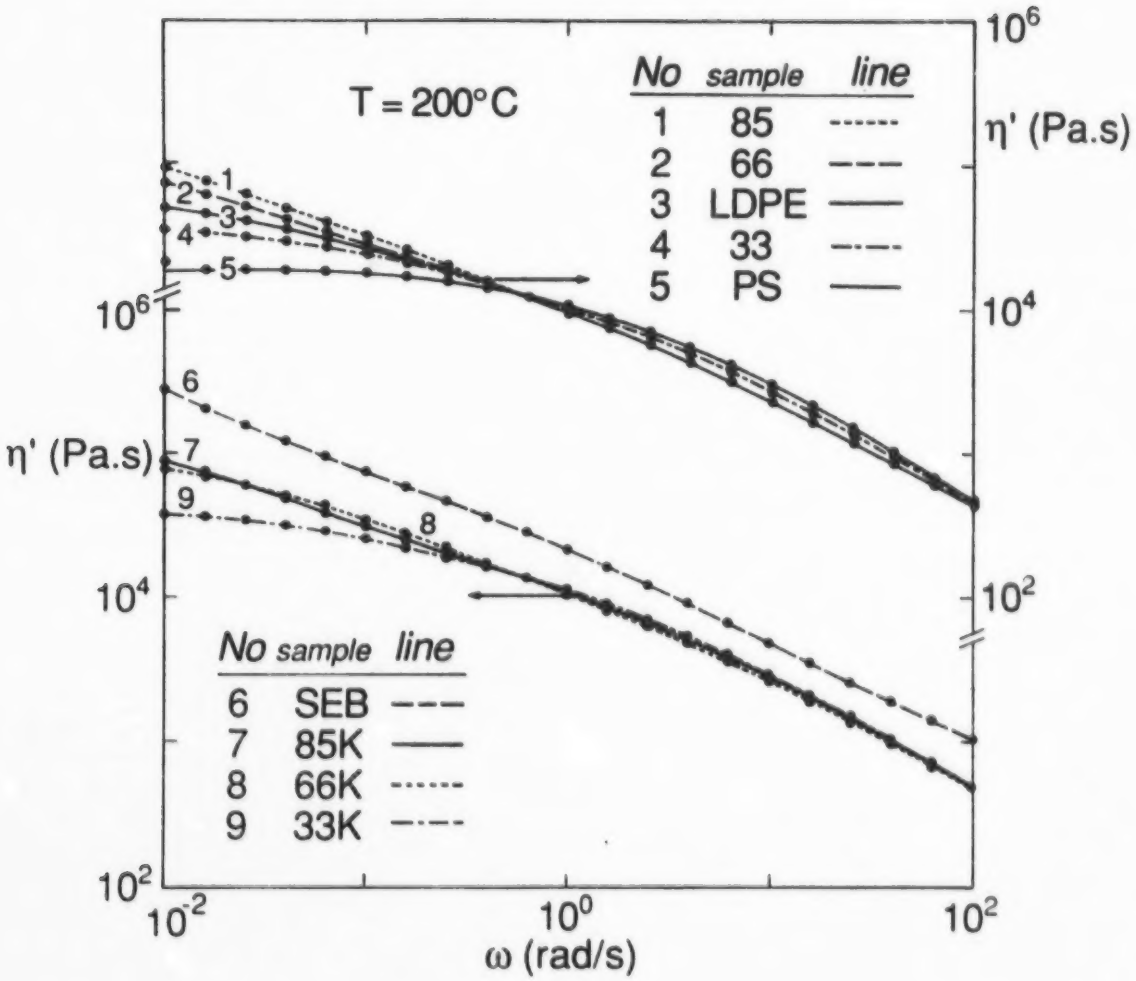

Fig. 4 Dynamic viscosity, $\eta'_a = G''_a/\omega$, vs. ω at 200°C for samples without (upper curves) and with SEB. Composition of the samples is given in Table 2.

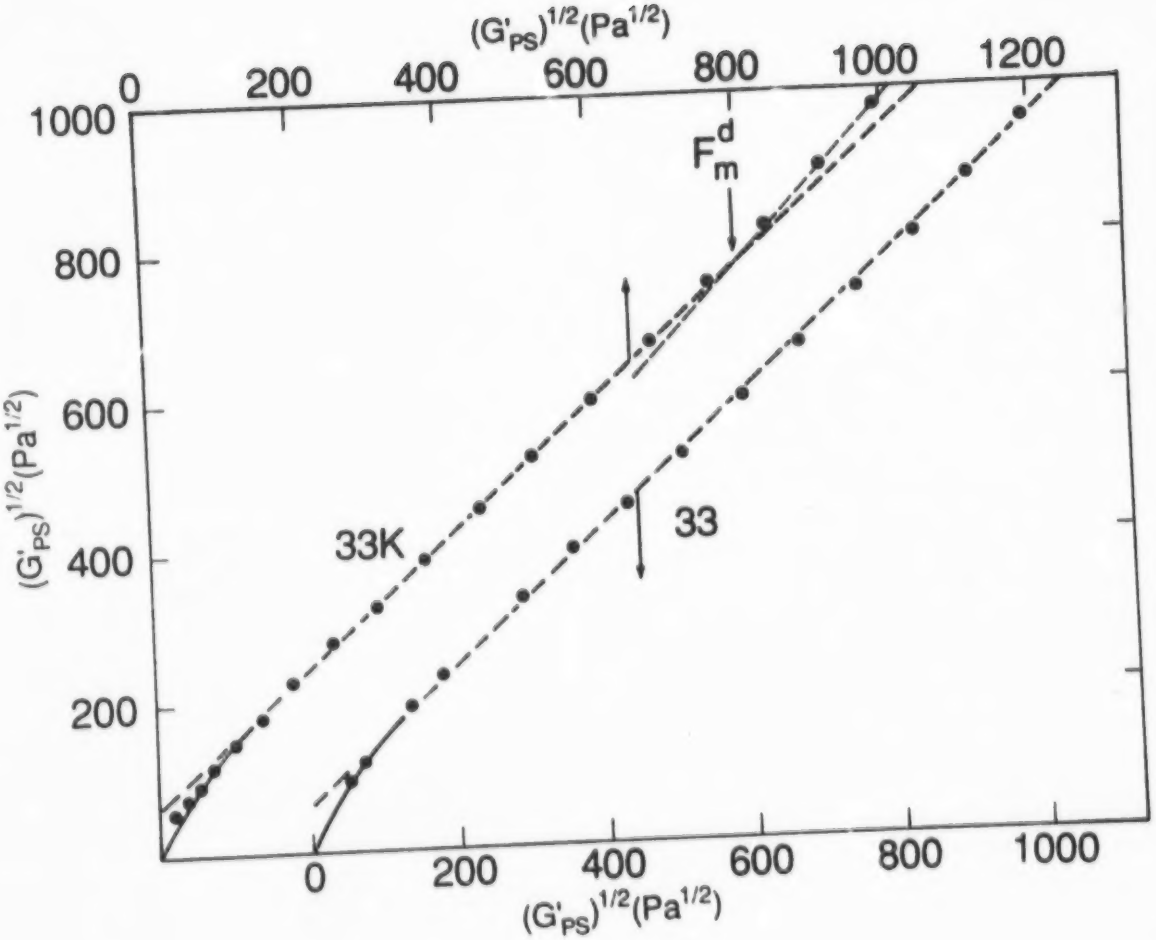

Fig. 5 Modified Casson plot, Eq (1), for storage modulus of blends 33K and 33 (with and without SEB, respectively). Note that $F = G'_a$ and for F_m the G' of matrix polymer, PS, was taken. The yield stress was calculated from the initial straight-line portion of the dependence, below the $(G'_{PS})^{\frac{1}{2}}$ value, marked as F_m^d. The curved portion starting at the origin was computed from Eq (2).

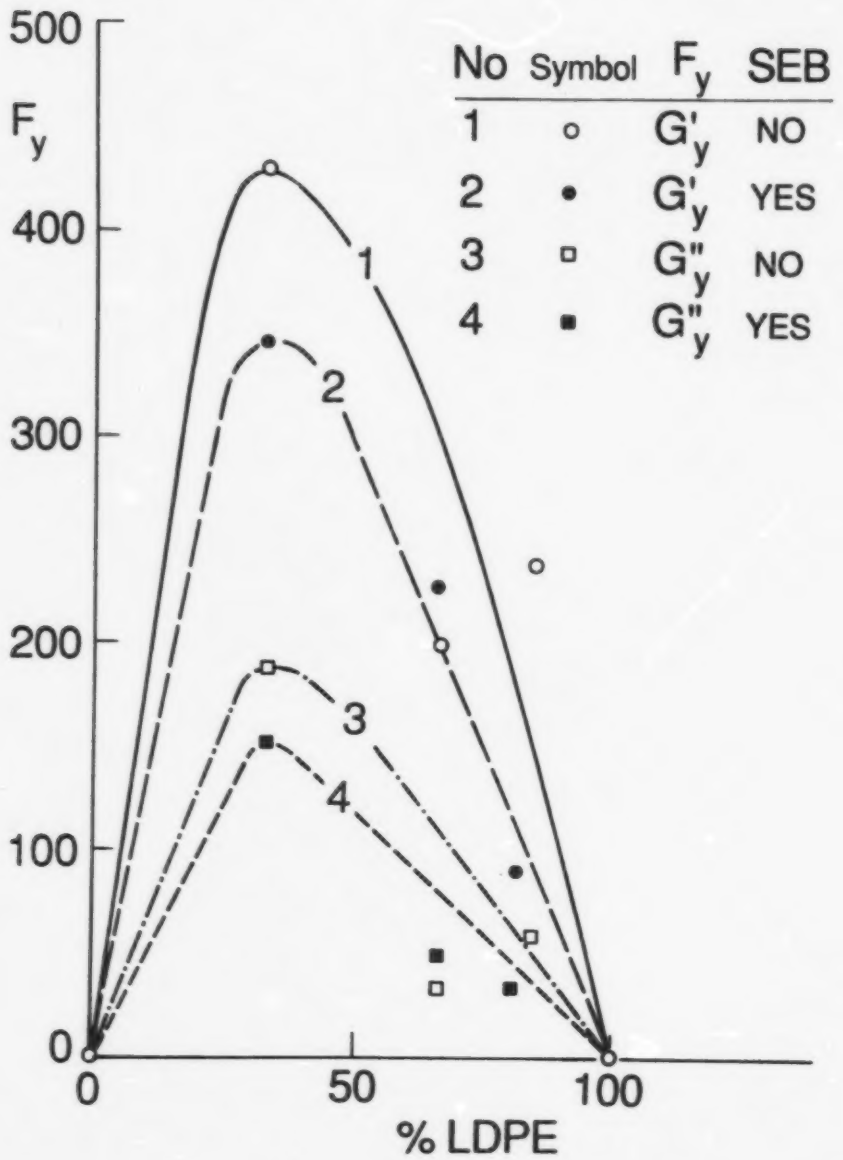

Fig. 6 The yield stress vs. composition for LDPE/PS blends. Curves 1 and 2 refer to yield in G'_a for blends without and with SEB, respectively, whereas curves 3 and 4 refer to yield in G''_a for the same blends. Points - experimental, lines - drawn to help the eye.

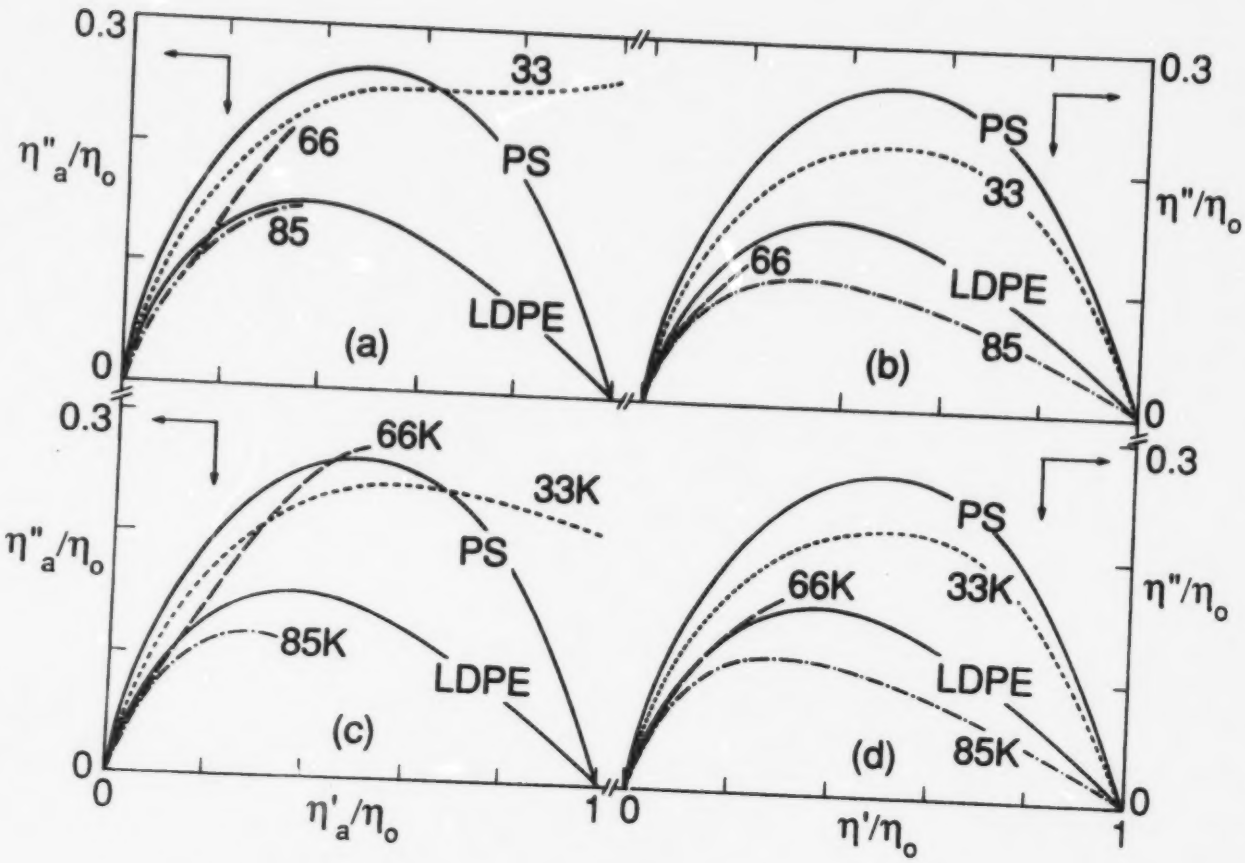

Fig. 7 The reduced Cole-Cole plot of: (a and c) apparent data for blends without and with SEB, respectively and for (b and d) corrected for the yield stress data of the same systems.

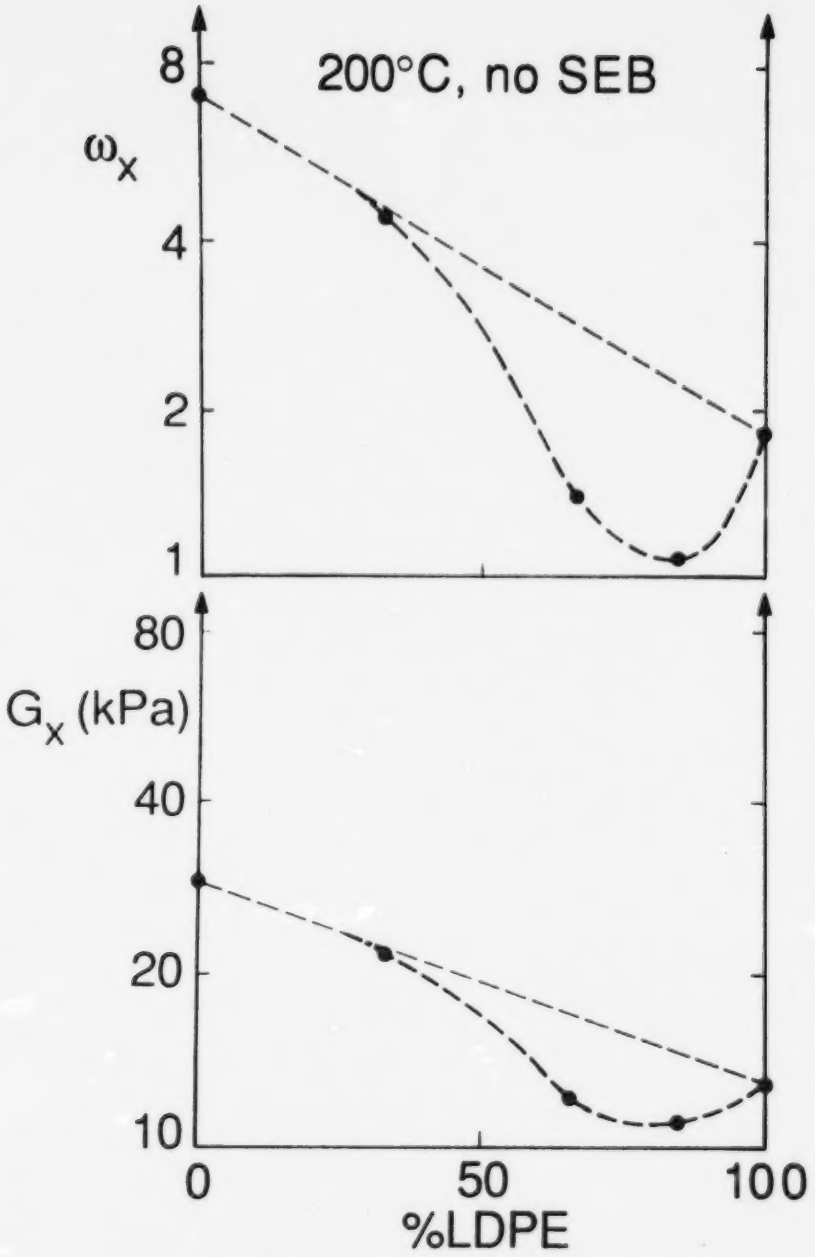

Fig. 8 Cross-point coordinates at 200°C vs. LDPE content for blends without SEB.

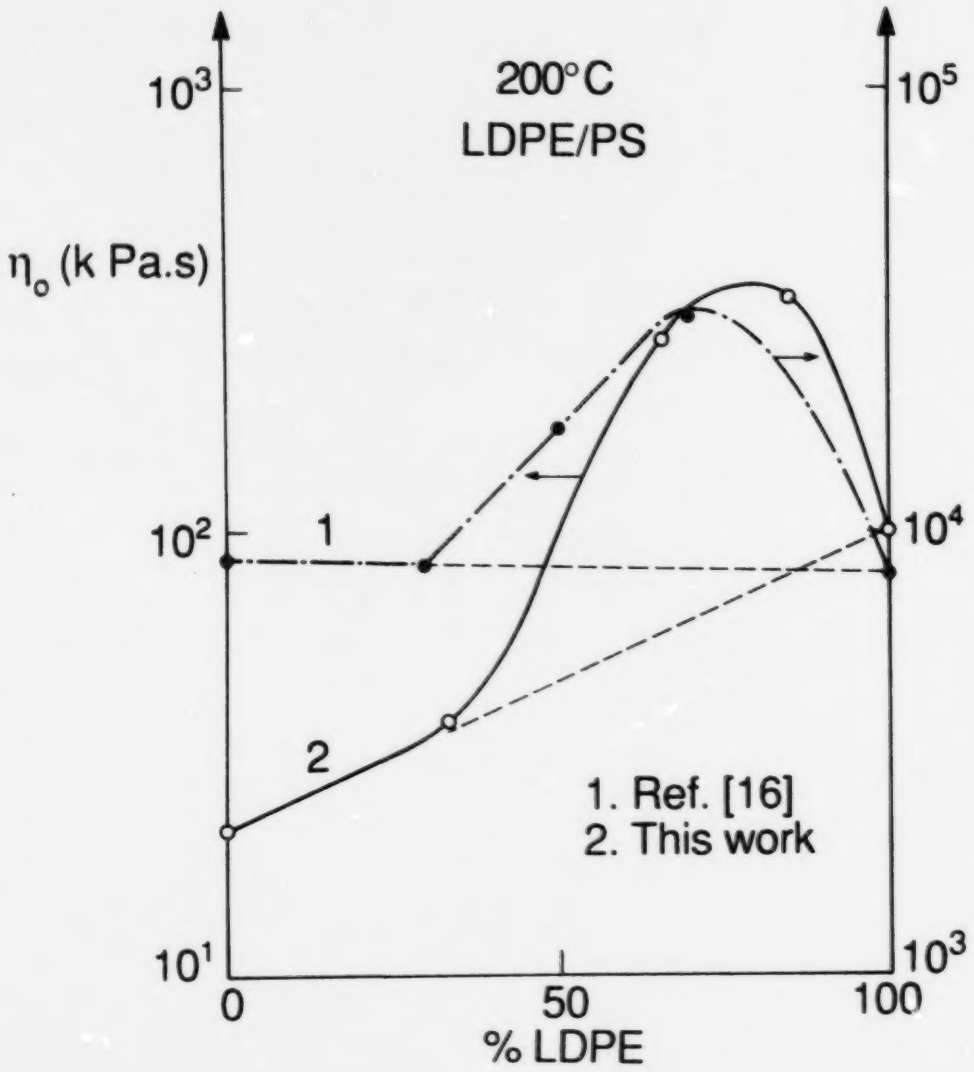

Fig. 9 Zero-shear viscosity at 200°C vs. LDPE content for two component LDPE/PS blends. Data from [16] are also shown.

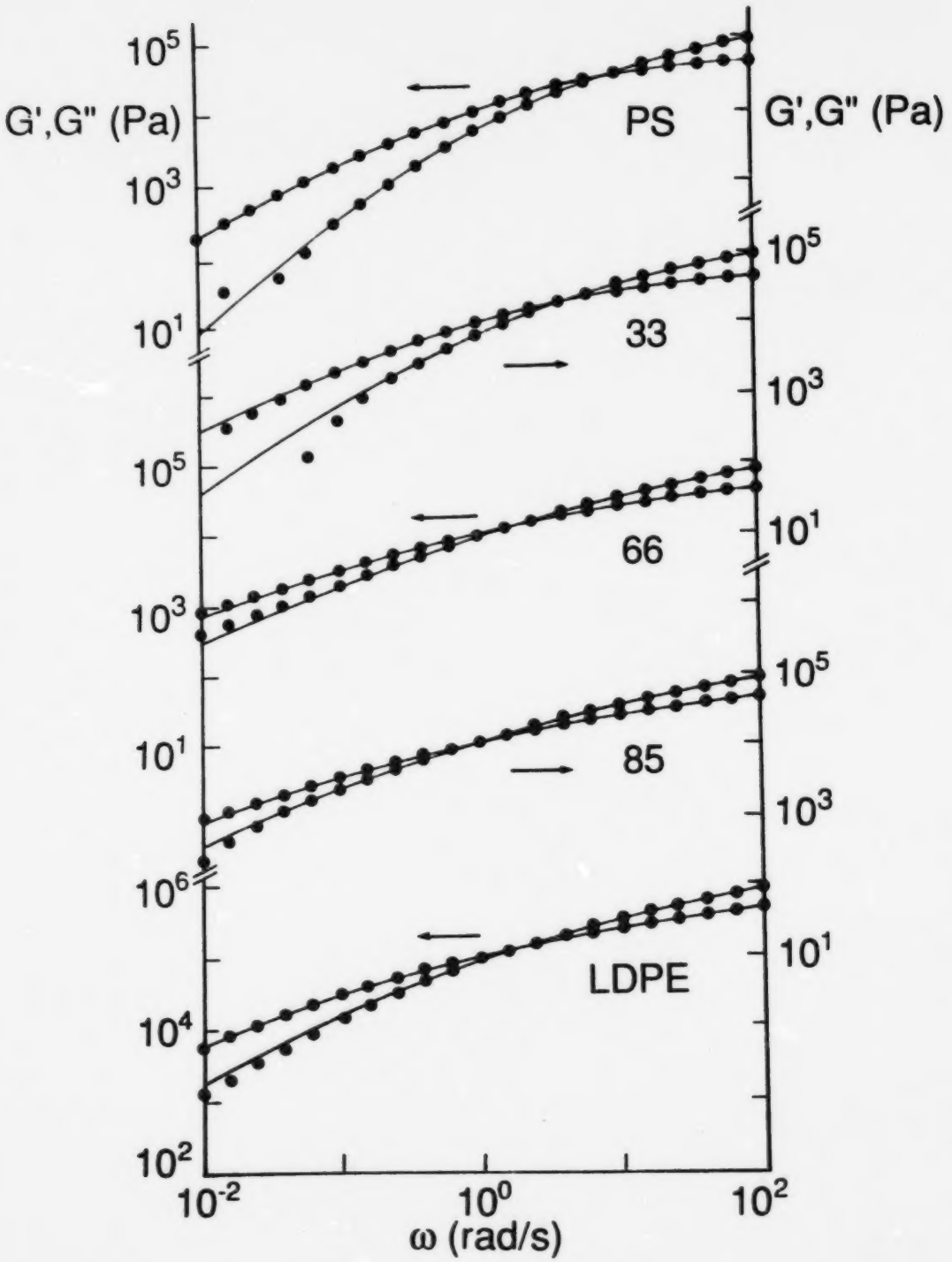

Fig. 10 Comparison between computed from the relaxation spectrum (lines) and measured (points) values of the shear moduli for LDPE/PS blends.

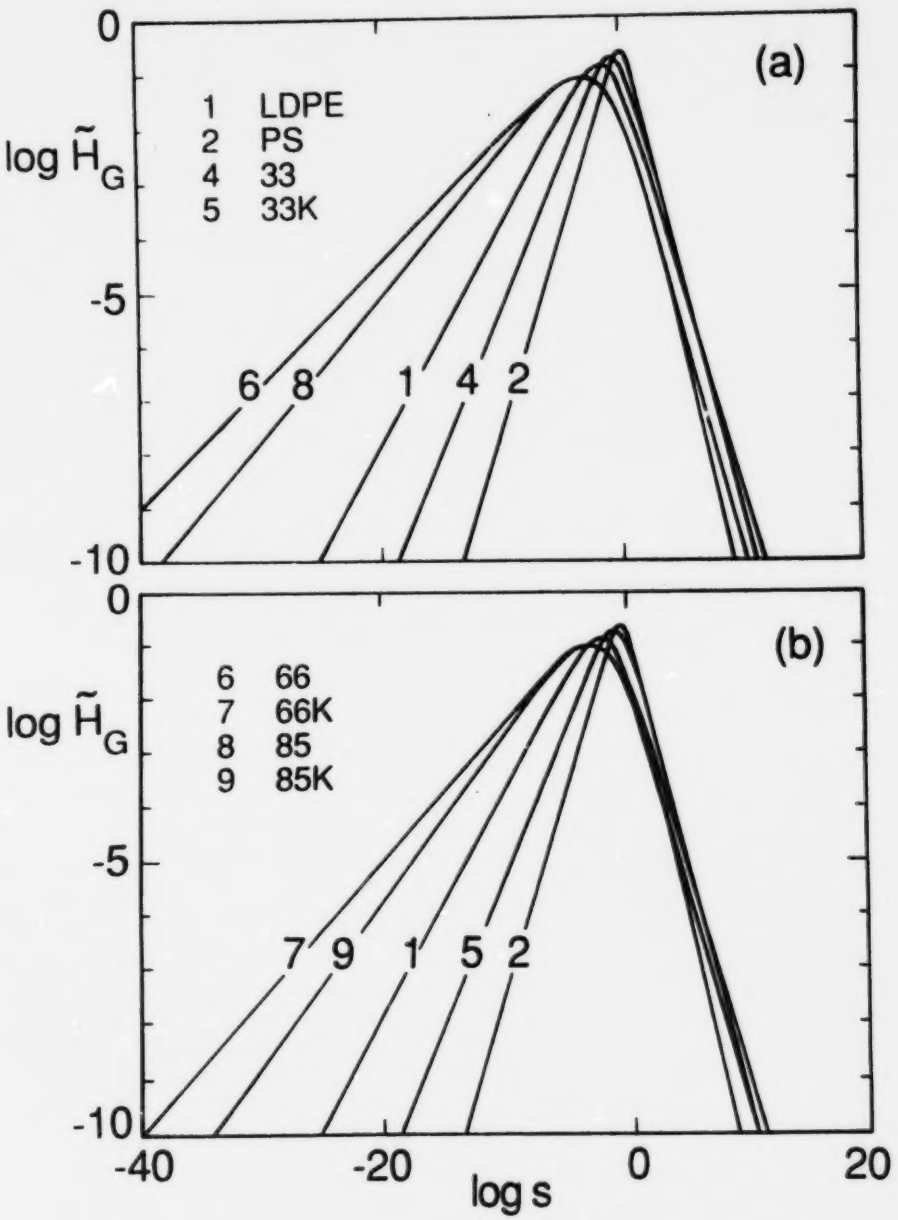

Fig. 11 Reduced frequency relaxation spectrum for (a) two component LDPE/PS blends, and for those with 5 wt% of SEB (b).

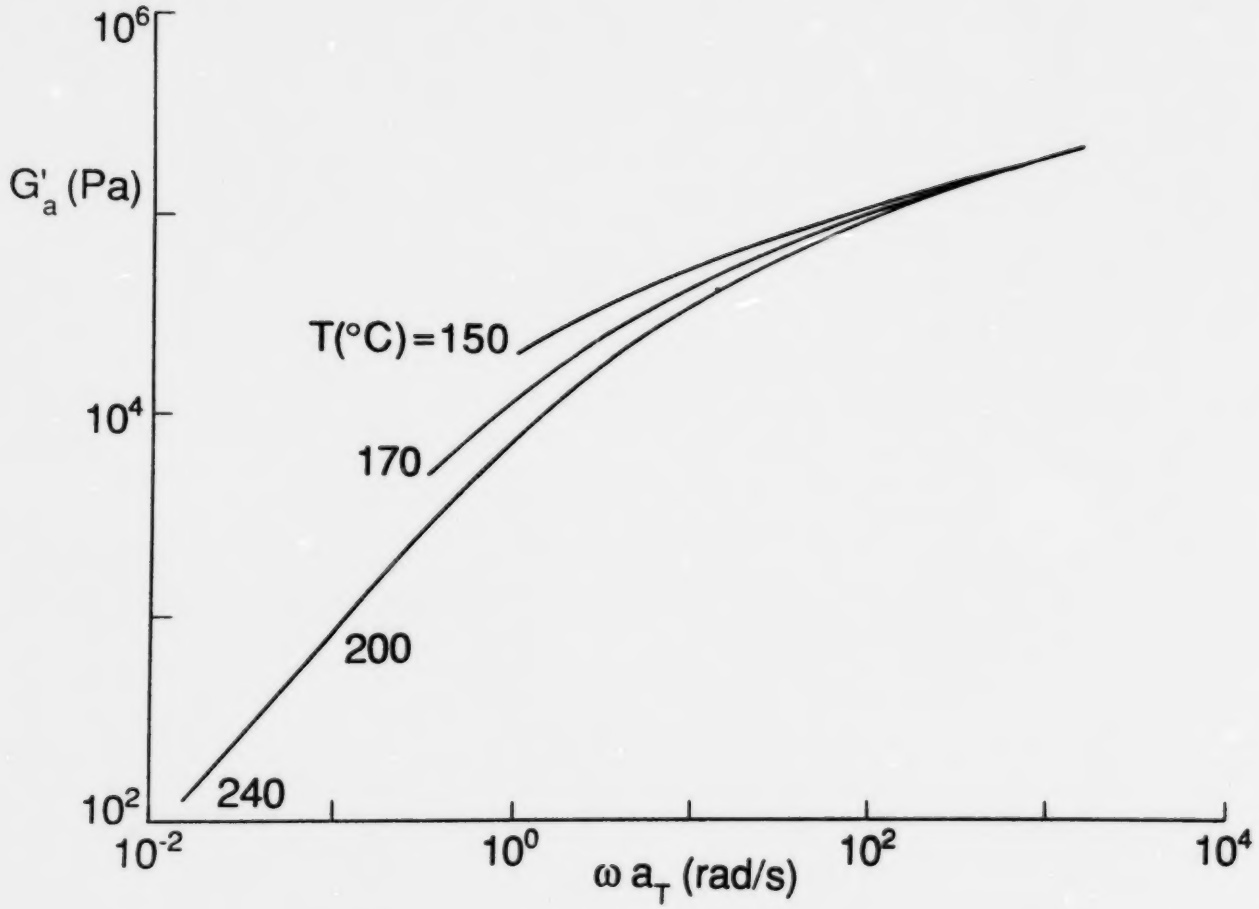

Fig. 12 Attempt of generation of the time-temperature superposition of apparent storage modulus, G'_a, for blend 33 at T = 150, 170, 200 and 240°C by horizontal shifting. Note good superposition for data at 200 and 240°C and lack of it at 150 and 170°C. The $a_T = a_T(T, \omega=100)$ was determined.

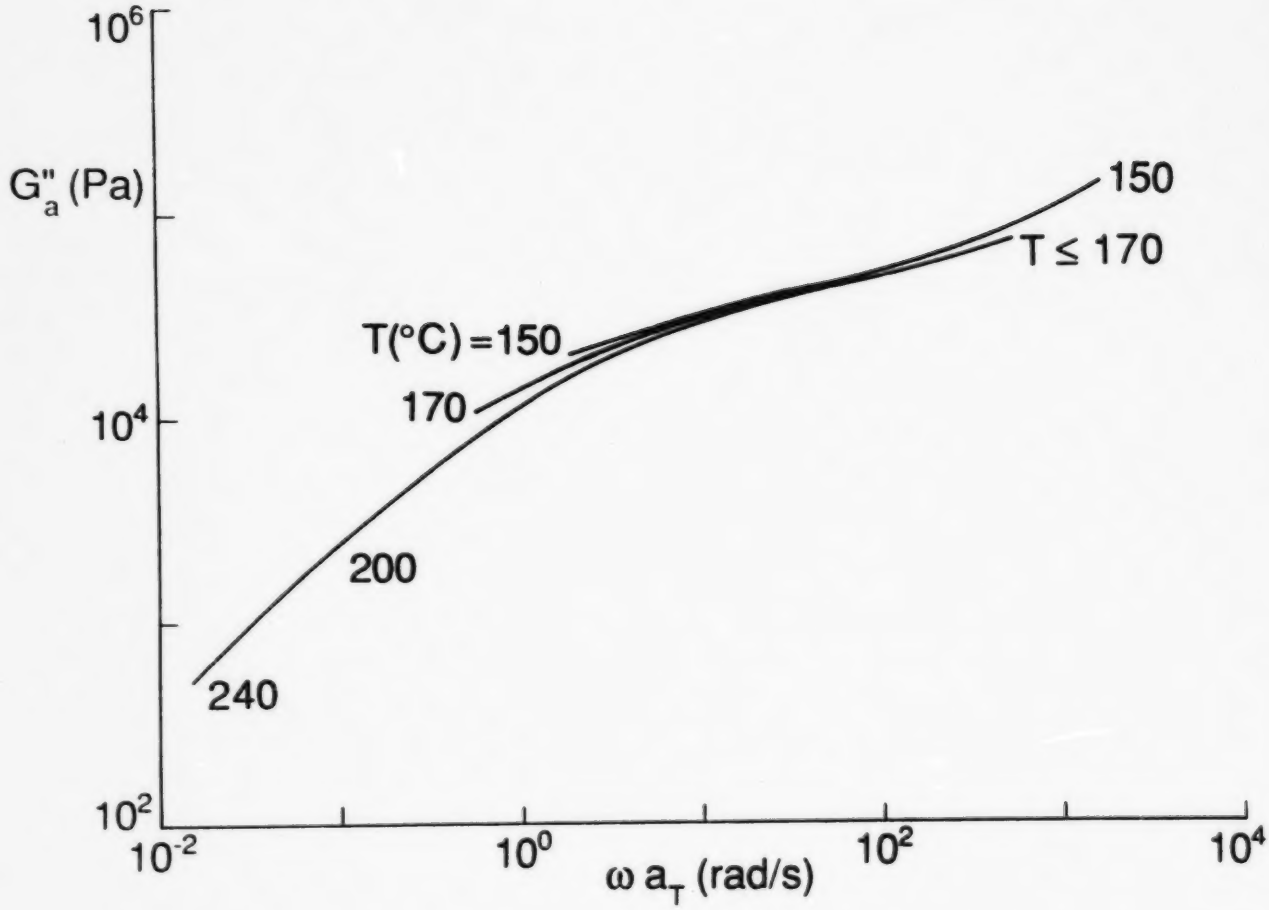

Fig. 13 Time-temperature superposition of the apparent loss modulus, G''_a, for blend 33 obtained by plotting its values vs. ωa_T, where a_T is the empirical shift factor determined in Fig. 12.

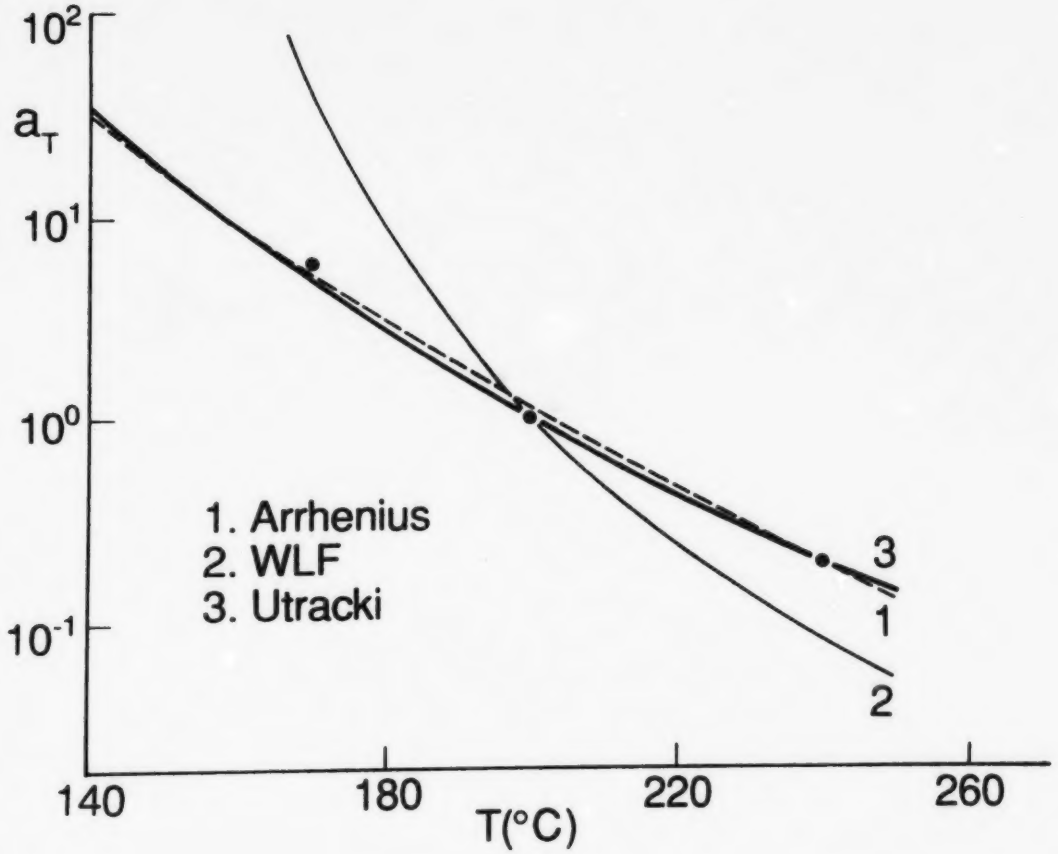

Fig. 14 Temperature dependence of the experimental shift factor, $a_T = a_T(T, \omega=100)$, for blend 33 (points). The curves 1 to 3 represent the best fit of the Arrhenius, WLF and Utracki equation, respectively.

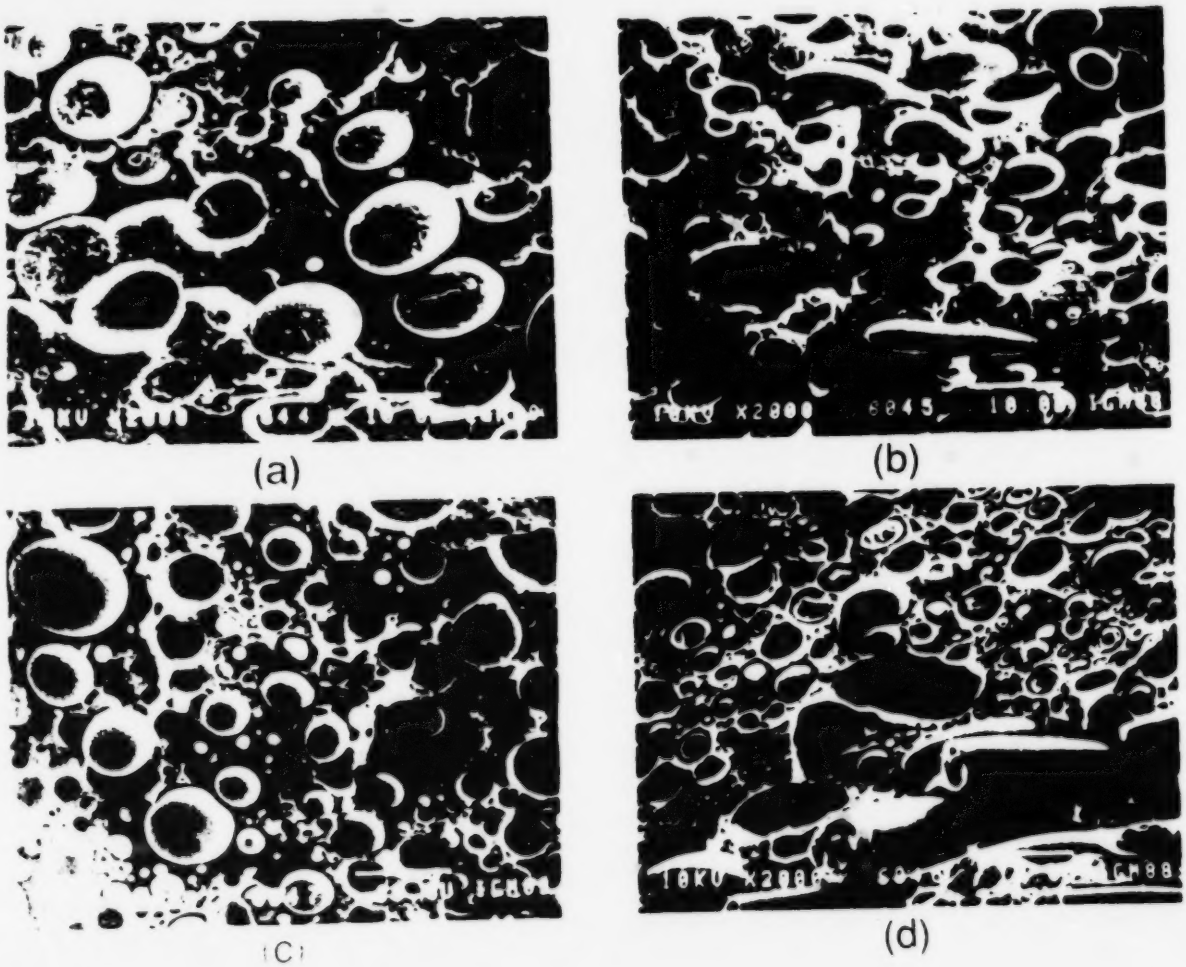

Photo 1 The scanning electron micrographs of blend 66K at rim of the RMS specimen: (a) prior to testing, (b) after 30 min at ω = 0.1 rad/s, T = 200 °C, and (c) after 18 sec at ω = 10 rad/s, T = 200°C.

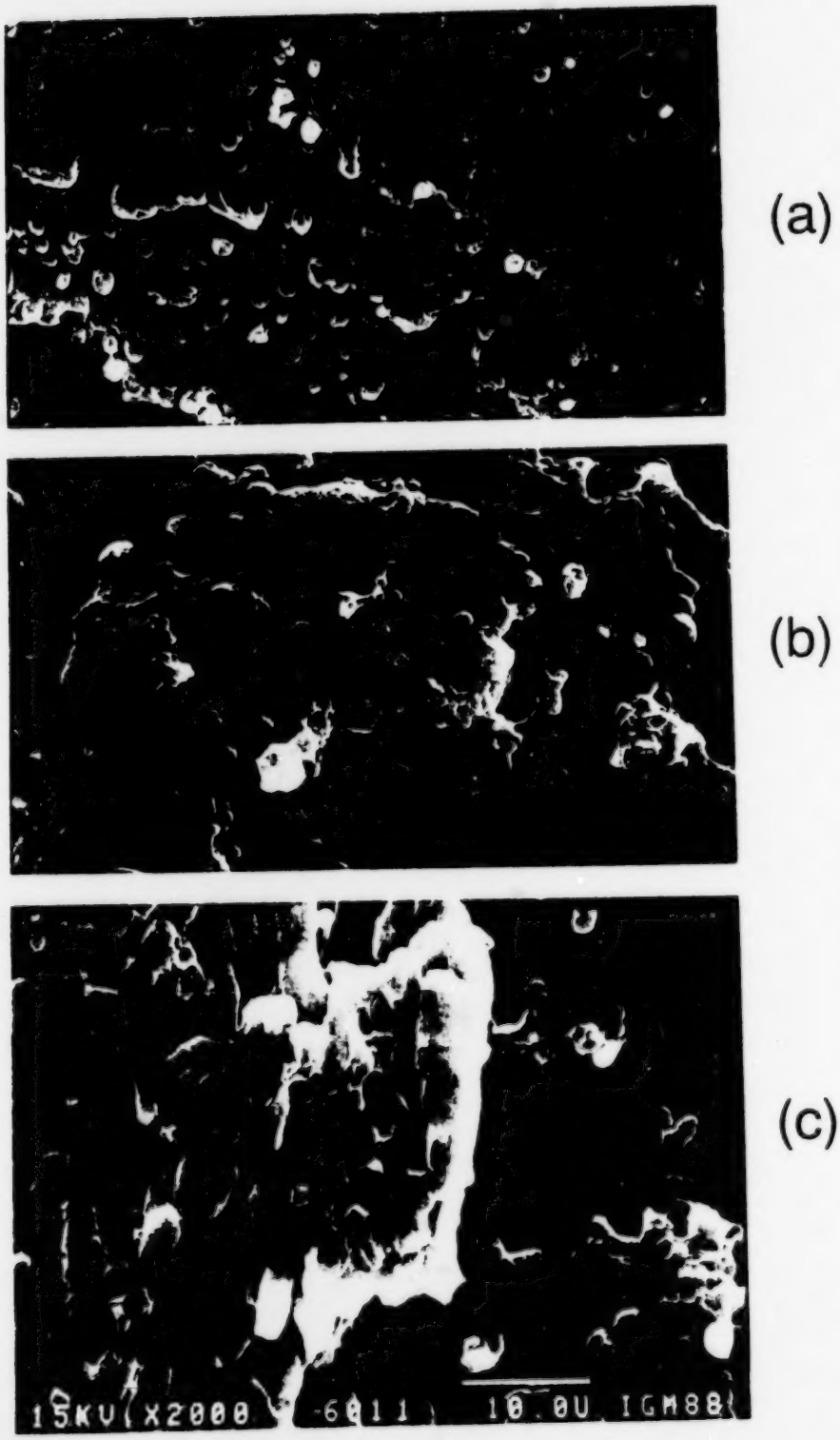

Photo 2 The scanning electron micrographs of blend 66 at the center of RMS parallel plates geometry (top) and at the edge. The test frequency